MedChemComm

CONCISE ARTICLE

Cite this: *Med. Chem. Commun.*, 2015, **6**, 677

Enantiomeric resolution of [(2,2-diphenyl-1,3-dioxolan-4-yl)methyl](2-phenoxyethyl)amine, a potent α_1 and 5-HT_{1A} receptor ligand: an *in vitro* and computational study

Silvia Franchini,*[a] Annamaria Baraldi,[a] Claudia Sorbi,[a] Federica Pellati,[a] Elena Cichero,[b] Umberto M. Battisti,[a] Piero Angeli,[c] Antonio Cilia[d] and Livio Brasili*[a]

Received 25th October 2014,
Accepted 19th December 2014

DOI: 10.1039/c4md00484a

www.rsc.org/medchemcomm

In this paper, the enantiomers of (±)-**1**, previously studied as α_1 and 5-HT_{1A} ligands, were prepared both by resolution of the racemate and asymmetric synthesis. The enantiomeric purity and absolute configuration were determined by means of HPLC and polarimetric analysis. Enantiomers were evaluated for *in vitro* 5-HT_{1A} and α_1 receptor affinity by binding and functional assays. Results indicate that the two enantiomers are almost equally potent at 5-HT_{1A} and α_1 receptor systems and, contrary to WB 4101, the stereoselectivity is poor. As further support to these experimental findings, molecular docking studies on the two enantiomers of (±)-**1** have been performed and a comparison with those obtained for 5-HT_{1A} potent agonist (*R*)-flesinoxan and α_{1d} antagonist (*S*)-WB 4101 has been drawn.

Introduction

The α_1 adrenergic receptors (α_1 adrenoceptors) play a key role in the modulation of the activity of the sympathetic nervous system, thus they represent a target for many therapeutic agents. α_1 adrenoceptors are divided into at least three subtypes named α_{1a} (α_{1A}), α_{1b} (α_{1B}), and α_{1d} (α_{1D}), with upper and lower cases indicating the native and recombinant receptors, respectively.[1,2] α_1 antagonists have been used to treat hypertension and they are considered the first-line therapy for the treatment of lower urinary tract symptoms associated with clinical benign prostatic hyperplasia.[3] 5-HT_{1A} is, to date, one of the most studied serotonin (5-HT) receptor subtypes and it represents a target for neurological research and drug development. It is generally accepted that 5-HT_{1A} is involved in anxiety and depression; recently, it has been suggested that 5-HT_{1A} agonists have neuroprotective properties,[4] whereas 5-HT_{1A} antagonists could be useful in the treatment of Alzheimer's disease.[5]

5-HT_{1A} and α_1-adrenergic receptors belong to the G-protein-coupled receptor (GPCR) superfamily and despite their distinct pharmacology they show a substantial similarity (approximately 45% identity) in their transmembrane amino acid sequence.[6] As a consequence, a number of 5-HT_{1A} ligands bind to α_1-adrenergic receptors with high affinity.

In our previous studies, we performed structure–activity relationship (SAR) analysis on a series of compounds derived from structural modifications of WB 4101, a prototype of the well-known class of α_1-adrenoceptor antagonists (benzodioxanes).[7,8] We have reported the discovery of the dioxolane derivative (±)-**1** (Fig. 1), and evaluated the binding to α_1 and 5-HT_{1A} receptors. It was found that (±)-**1** is a selective antagonist, at least in functional studies, for the α_{1D} subtype. However, it displays high affinity for the 5-HT_{1A} receptor with consequently no selectivity, compared to the α_1-adrenergic

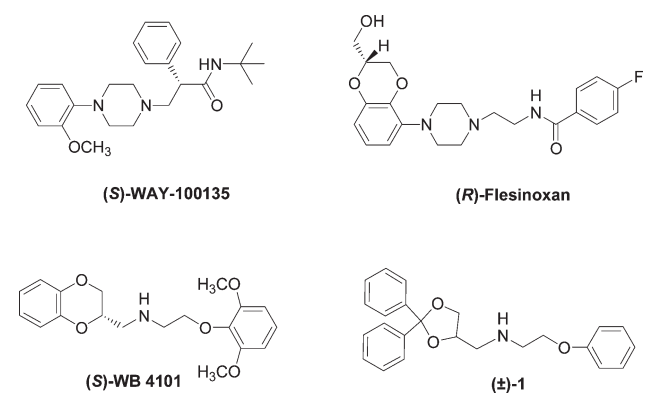

Fig. 1 Chemical structures of (*S*)-WAY-100135, (*R*)-flesinoxan, (*S*)-WB 4101 and (±)-**1**.

[a] *Dipartimento di Scienze della Vita, Università degli Studi di Modena e Reggio Emilia, Via Campi 183, 41125 Modena, Italy. E-mail: brasili.livio@ unimore.it; Fax: +39 059 205 5131; Tel: +39 059 205 5139*
[b] *Dipartimento di Farmacia, Università degli Studi di Genova, Viale Benedetto XV 3, 16132 Genova, Italy*
[c] *Dipartimento di Scienze Chimiche, Università degli Studi di Camerino, Via S. Agostino 1, 62032 Camerino, Italy*
[d] *Divisione Ricerca e Sviluppo, Recordati S.p.A., Via Civitali 1, 20148 Milano, Italy*

system. In an extension of this work, we thought that it would be interesting to obtain the single enantiomers of compound (±)-**1** in order to evaluate the possible stereospecific interaction and thus the relative contribution of these enantiomers to the binding with the 5-HT_{1A} and α_1-adrenergic receptors. The 5-HT_{1A} and α_1-adrenergic receptors have, in fact, demonstrated a considerable influence of chirality in their interactions with ligands. Some examples are represented by the potent 5-HT_{1A} antagonist WAY 100135, whose affinity resides predominantly in the (*S*)-enantiomer, being 28 times more potent than the (*R*)-enantiomer[9,10] or by the 5-HT_{1A} potent agonist flesinoxan for which the (*R*)-enantiomer is 10 times more potent than the (*S*)-enantiomer.[11,12] Moreover, some studies on WB 4101 and some analogues have demonstrated that the (*S*)-isomer is more potent than its (*R*) counterpart at α_1-adrenoceptor subtypes.[13,14]

In addition, in order to rationalize the obtained results, molecular docking studies on compounds (±)-**1** were performed, using the 5-HT_{1A} and α_{1d} homology models previously built by us.[15] Successively, the "*in silico*" predicted binding mode was compared with that of the 5-HT_{1A} potent agonist (*R*)-flesinoxan and α_{1d} antagonist (*S*)-WB 4101.

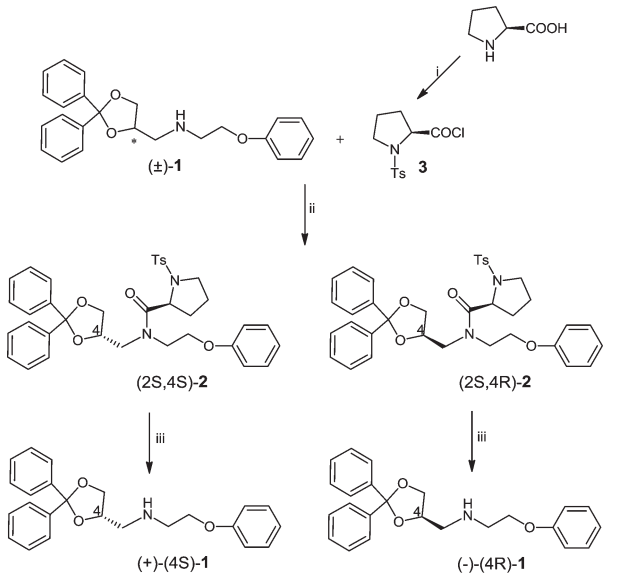

Scheme 1 Reagents and conditions: i) a. Na_2CO_3, TsCl, H_2O, 0–5 °C. b. $SOCl_2$, toluene, reflux; ii) Py, CH_2Cl_2, 0 °C to reflux followed by chromatographic separation; iii) C_2H_5ONa, C_2H_5OH, reflux.

Results and discussion

Enantioseparation of (±)-1 and determination of the optical purity

Enantioseparation is often feasible by fractional crystallization: the reaction of a racemic acid or base with an optically active base or acid gives a pair of diastereomeric salts which can be separated through preferential precipitation. Our attempts on fractional crystallization of (±)-**1** in the presence of (L)(+)-tartaric or (D)(−)-mandelic acid as resolving agents, however, were investigated with no success. Another commonly used method for the resolution of racemates involves enantioseparation of the optical isomers using semipreparative chiral HPLC. Unfortunately, using a chiral semipreparative column (Chiralcel OD), only a partial separation was achieved (R_s <1.5) under several chromatographic conditions. Thus in order to obtain enantiomerically pure (*R*)-**1** and (*S*)-**1**, we focused on the conversion of the enantiomers into diastereomers and the subsequent separation of the diastereomeric mixture by ordinary separation techniques, such as chromatography. Racemate (±)-**1** was prepared by *N*-alkylation of 2-phenoxyethylamine with 4-chloromethyl-2,2-diphenyl-1,3-dioxolane according to our previously published procedure.[7] Resolution of (±)-**1** was achieved by conversion of the two enantiomers into their diastereomeric amides.[13] (*S*)-Proline was *N*-tosylated and then used as a chiral resolving agent after activation of the carboxylic group into the corresponding acyl chloride (**3**) (Scheme 1).[16] Thus *N*-tosyl-(*S*)-prolyl chloride (**3**) was allowed to react with the amino group of (±)-**1** to give a pair of diastereomeric amides, (2*S*,4*S*)-**2** and (2*S*,4*R*)-**2**, which were separated by flash chromatography on a silica gel column, using cyclohexane/ethyl acetate 70/30 (v/v) as the mobile phase.

Collected fractions were analysed by HPLC, using a Speri-5 silica gel column (250 × 4.6 mm, 5 μm), mobile phase: cyclohexane/ethyl acetate 70/30 (v/v), flow rate: 1 ml min^{-1}, column temperature: 20 °C, injection volume: 5 μL; UV detection at 254 nm, and pooled. As shown in Fig. 2a, a good resolution between the peaks of the two diastereomers, (2*S*,4*S*)-**2** and (2*S*,4*R*)-**2**, was obtained in a short analysis time (t_R = 9.9 min for the first eluted isomer and 13.4 min for the last one; resolution (R_s) = 5.89; selectivity (α) = 1.34). In order to determine the diastereomeric purity of the pooled fractions, the diastereomeric excess (d.e.) was calculated from the integrated peak areas of the two diastereomers. The resulting d.e. was found to be >99% for both isomers (Fig. 2b, c).

The separated isomers were characterized by means of HPLC, HR-MS and ^{1}H and ^{13}C NMR analysis. The ^{1}H NMR spectra of (2*S*,4*S*)-**2** and (2*S*,4*R*)-**2** showed very little differences (<0.01 ppm) with regard to the chemical shift values of the protons bound to the proline chiral carbon and those of the methyl group of the tosyl moiety. Moreover, the ^{1}H-NMR spectrum of a single isomer (2*S*,4*S*)-**2** or (2*S*,4*R*)-**2** results in a mixture of two conformers, (*E*) and (*Z*), due to the restricted rotation about the amide C–N bond, making the spectral assignments quite difficult. The amide C–N bond in fact is locked at room temperature as if it were a double bond (Fig. 3). In particular, in the case of the first eluted isomer (2*S*,4*S*)-**2**, the (*Z*):(*E*) ratio was 1 : 0.8 while 1 : 0.3 was found for the last eluted isomer (2*S*,4*R*)-**2**, as determined by NOESY experiments (see below) (*E*–*Z* notation refers to Cahn–Ingold–Prelog priority rules). The different ratios are probably due to the steric hindrance of *cis* tosyl-proline and 2,2-diphenyl-1,3-dioxolan-4yl-methyl groups. As the temperature increases, the energy available is sufficient to overcome the rotational barrier and allow the two conformers to interchange.

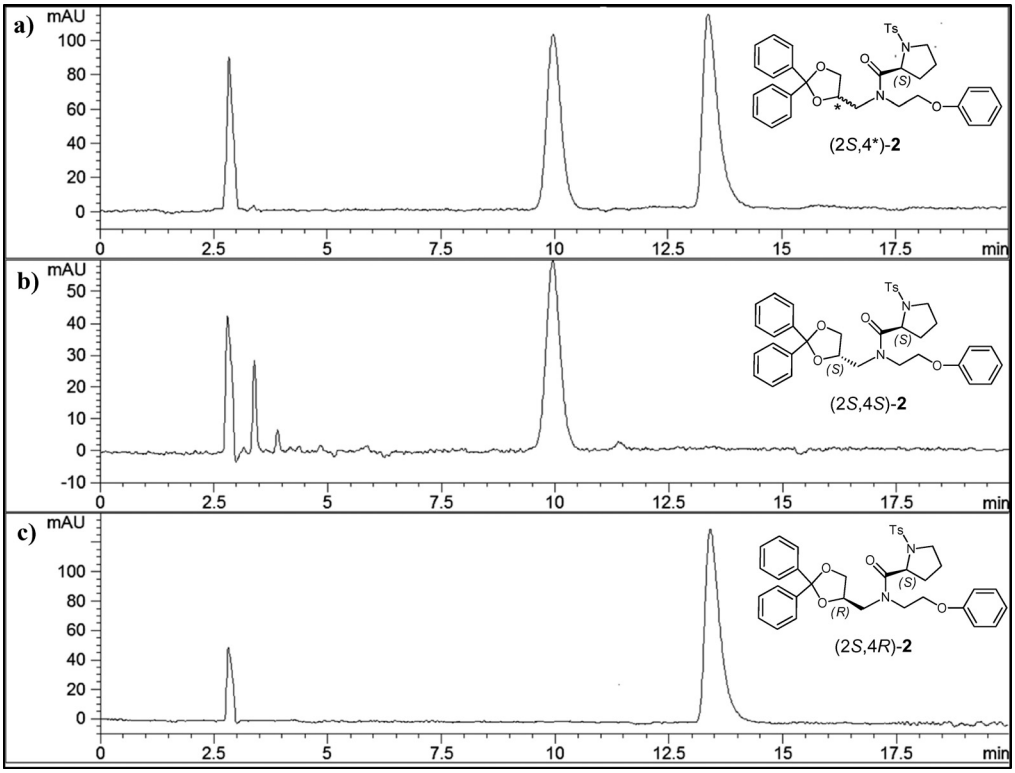

Fig. 2 HPLC analysis of a) the diastereomeric amides (2*S*,4*S*)-**2** (t_R = 9.9 min) and (2*S*,4*R*)-**2** (t_R = 13.4 min); b) first eluted isomer (less polar); c) second eluted isomer (more polar). Solvent peak (t_R = 2.59 min) and impurities are eluted between 3.0–3.5 min. Chromatographic conditions: column: Speri-5 silica gel (250 × 4.6 mm, 5 μm); mobile phase: cyclohexane/ethyl acetate, 70/30 (v/v); flow rate: 1 ml min^{-1}; column temperature: 20 °C; injection volume: 5 μL; detection: UV at 254 nm.

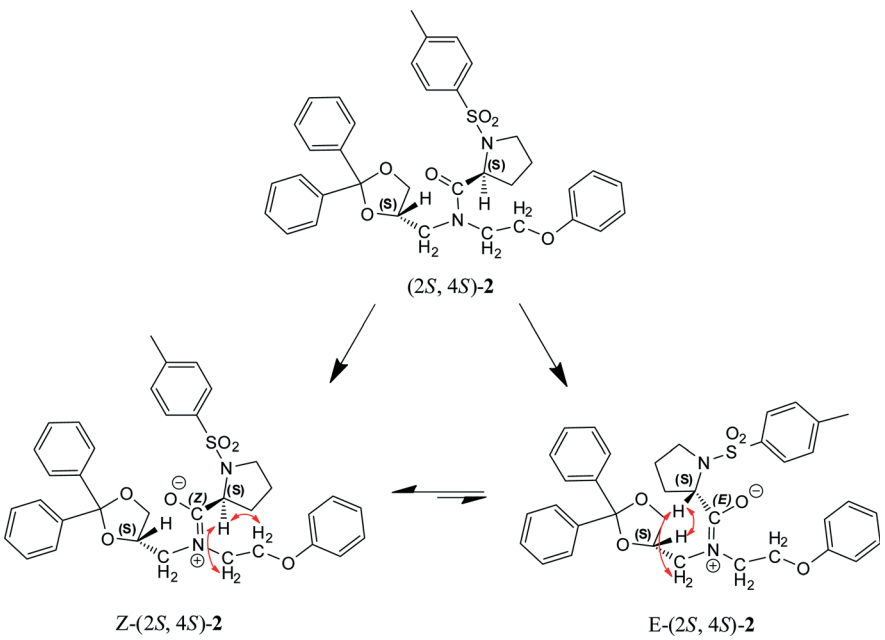

Fig. 3 Representation of the two conformers of the diastereomeric amide (2*S*,4*S*)-**2** observed in ^{1}H-NMR experiments. Red arrows indicate the observed positive NOE effect.

In correspondence with the coalescence temperature (100 °C), the chemical shifts of the (*E*) and (*Z*) conformers vary up to a mean value comprised between that of the two forms weighted by their abundance. Nuclear Overhauser Effect Spectroscopy experiments (NOESY) were also carried out to identify cross peaks originating from conformational

exchange. In particular, for small molecules having long correlation time, the phase of the peak can be used as evidence: with the diagonal signal phased 'down', the chemical exchange cross peak is also phased 'down', as observed for the H4 and H5-dioxolane, and H2 proline (*E*)/(*Z*) protons. Moreover, NOESY experiments have enabled us to assign the (*E*)/(*Z*) configuration. In particular, the (*Z*) conformer showed two cross peaks originating from the NOE effect (opposite sign compared to the diagonal) between the H2-proline proton and both methylene groups of the phenoxyethyl chain; this is not true for the (*E*) isomer. Conversely, the (*E*) conformer showed a positive NOE effect between the H2-proline and H4-dioxolane proton and between the H2-proline and CH_2–N proton, as depicted in Fig. 3 (red arrows). The same correlations have been observed for the two conformers of the diastereomeric amide (2*S*,4*R*)-**2**.

The separated diastereomers (2*S*,4*S*)-**2** and (2*S*,4*R*)-**2** were then transformed into the corresponding enantiomers (*S*)-**1** and (*R*)-**1** by reaction with sodium ethoxide.[16] To confirm that racemization does not occur in the course of the reaction, a certain amount of enantiomer was converted into the corresponding amide of *N*-tosyl-(*S*)-proline (Scheme 2) and HPLC analysis was carried out, using the same experimental conditions mentioned in Fig. 2. For both epimers, racemization was excluded since the diastereomeric excess was >99% (data not shown).

Determination of the absolute configuration. The absolute configuration of the two optical isomers (*S*)-**1** and (*R*)-**1**, obtained by resolution of the racemate (±)-**1**, was assigned using a comparison of the optical rotation with the authentic samples (+)-(*S*)-**1′** and (−)-(*R*)-**1′**, which were prepared by asymmetric synthesis, starting from the commercially available chiral alcohols (−)-(*R*)-3-chloro-1,2-propanediol (e.e. 98%) and (+)-(*S*)-3-chloro-1,2-propanediol (e.e. 97%), respectively, following the procedure previously reported for the synthesis of racemate (±)-**1** (Scheme 3).[7] The conversion of the chloro derivative (*R*)-**4** into the corresponding amine (+)-(*S*)-**1′** causes the inversion of notation (*R* to *S* form and *vice versa*) due to the priority changes around the stereocenter.

Table 1 illustrates the specific optical rotation of enantiomers (*S*)-**1′** and (*R*)-**1′**, obtained from the asymmetric synthesis, and the specific optical rotation of enantiomers (*S*)-**1** and

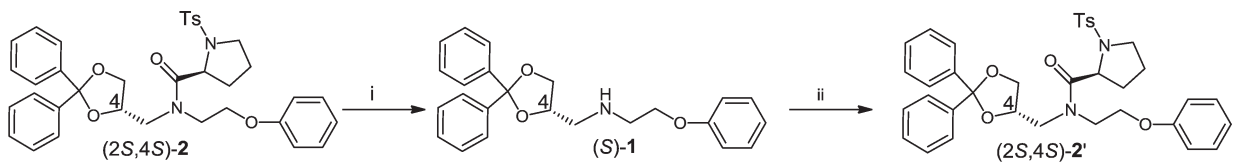

Scheme 2 Reagents and conditions: i) C_2H_5ONa, C_2H_5OH, reflux; ii) **3**, Py, CH_2Cl_2, 0–5 °C to reflux.

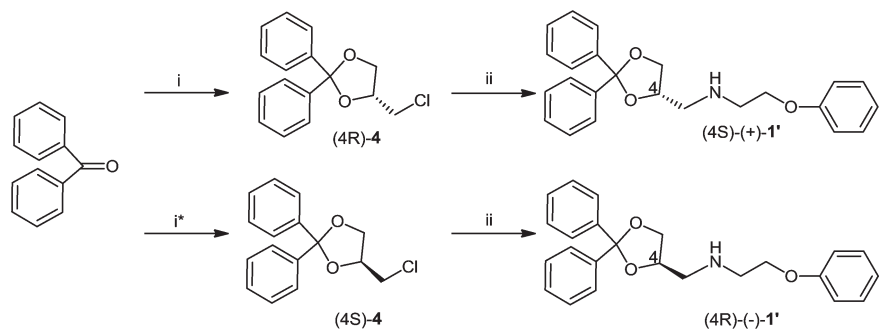

Scheme 3 Reagents and conditions: i) (2*R*)-(−)-3-chloro-1,2-propanediol, *p*-TSA, toluene, reflux; i*) (2*S*)-(+)-3-chloro-1,2-propanediol, *p*-TSA, toluene, reflux; ii) 2-phenoxy-ethylamine, 2-methoxy-ethanol, KI, reflux.

Table 1 Specific optical rotation $[\alpha]_D^{20}$ and $[\alpha]_{436}^{20}$ of enantiomers (*S*)-(+)-**1′** and (*R*)-(−)-**1′**, (*S*)-(+)-**1** and (*R*)-(−)-**1**, and (*S*)-(+)-3-chloro-1,2-propanediol and (*R*)-(−)-3-chloro-1,2-propanediol

Compounds	$[\alpha]_D^{20}$	$[\alpha]_{436}^{20}$	$[\alpha]_D^{20}$	$[\alpha]_{436}^{20}$	g ml^{-1c}
(*S*)-(+)-**1′**	+0.044	+0.107	+3.8	+9.4	0.011
(*R*)-(−)-**1′**	−0.044	−0.109	−3.7	−9.1	0.012
(*S*)-(+)-**1**	+0.039	+0.096	+3.9	+9.6	0.010
(*R*)-(−)-**1**	−0.037	−0.092	−3.7	−9.2	0.010
(*S*)-(+)-3-chloro-1,2-propanediol*[a]	+0.137	+0.275	+8.5	+16.9	0.016
(*R*)-(−)-3-chloro-1,2-propanediol*[b]	−0.085	−0.157	−8.5	−15.7	0.010

*Standards employed to test the accuracy of the measurements.[a] 97% pure. [b] 98% pure. [c] For enantiomers (*S*)-(+)-**1′** and (*R*)-(−)-**1′**, (*S*)-(+)-**1** and (*R*)-(−)-**1**, $CHCl_3$ was used as a solvent; for (*S*)-(+)-3-chloro-1,2-propanediol and (*R*)-(−)-3-chloro-1,2-propanediol, ethanol was used as a solvent.

(*R*)-**1**, obtained from the racemate (±)-**1**. Enantiomers (*S*)-**1** and (*R*)-**1** exhibit almost equal magnitude but opposite sign of specific optical rotation ($[\alpha]_{436}^{20}$ = +9.6 and −9.2, respectively), in agreement with the theory of optical activity. Enantiomers (*S*)-**1** and (*R*)-**1** showed a similar value of $[\alpha]_{436}^{20}$ when compared to the authentic samples (*S*)-**1′** and (*R*)-**1′** ($[\alpha]_{436}^{20}$ = +9.4 and −9.1, respectively). The specific rotation of the enantiomers of 3-chloro-1,2-propanediol was calculated as evidence proving the accuracy of the measurements. The enantiomers (*S*)-(+)-**1** and (*R*)-(−)-**1** were then treated with oxalic acid and the resulting oxalate salts were tested for biological activity on 5-HT_{1A} and α_1 receptors.

Structure–affinity and activity relationships

The pharmacological profile was initially evaluated by radioligand binding assays. Table 2 lists the affinity constants (pK_i) of enantiomers (*S*)-**1**, (*R*)-**1** and the racemate (±)-**1** for the 5-HT_{1A} receptor and for three α_1-adrenoceptor subtypes (α_{1a}, α_{1b}, α_{1d}) along with the 5-HT_{1A}/α_1 selectivities.

The *R*- and *S*-enantiomers and their racemate (±)-**1** bind preferentially to the 5-HT_{1A} receptor than to the three α_1 adrenergic subtypes with the *R*-form being the most selective (5-HT_{1A}/α_{1d} = 8).

While in the case of WB 4101, the *S*-enantiomer displays at least ten-fold higher 5-HT_{1A} affinity than its corresponding *R*-isomer,[17] the affinities for 5-HT_{1A} of the enantiomers of (±)-**1** are very similar, indicating the absence of stereospecific interaction of the chiral carbon at the 4 position of the 1,3-dioxolane ring in the binding process with this receptor. Both forms (*S*)-**1** and (*R*)-**1** behave as partial agonists for 5-HT_{1A}, with potency values (pD_2) of 7.45 and 6.85 and E_{max} values of 65 and 50, respectively. Concerning the α_1 receptor, the affinities of the *R*-enantiomer for the three subtypes are similar to that of the racemate (±)-**1**, indicating a small but consistent preference for the α_{1d} subtype. In terms of stereoselectivity, the *S*-isomer displays a lower affinity than the *R*-isomer, in particular for α_{1a} and α_{1b} receptors, thus paralleling, although to a lesser extent, the finding obtained with the enantiomers of WB 4101.[13] Both (*R*)-**1** and (*S*)-**1** display higher affinity for the α_{1d} receptor subtype with selectivity of approximately 2- and 4-fold for *R* and 9- and 8-fold for *S* over α_{1a} and α_{1b} receptors, respectively.

The antagonist potency and subtype selectivity of compound (±)-**1** and its single enantiomers were also determined for α_1-adrenoceptors on different isolated tissues. Table 3 illustrates the pharmacological results obtained for functional preparations such as prostatic vas deferens (α_{1A}), spleen (α_{1B}), and thoracic aorta (α_{1D}) of rat.

There is a correspondence between the binding and functional affinities for α_1-adrenoceptors; in fact, in both assays, *R*- and *S*-enantiomers exhibit higher affinity towards α_{1D} than α_{1A} and α_{1B}.

Moreover, selectivity values for α_1-adrenoceptor subtypes are higher in functional with respect to the binding assays, as a consequence of the lower affinities that the two isomers display for α_{1A} and α_{1B} receptors in functional tests.

As shown in Tables II and III, the enantioselectivity (*R*/*S*) to α_1-adrenoceptors is quite low. In the case of the α_{1D} receptor subtype, for which (*S*)-**1** and (*R*)-**1** exhibit the highest potency (pK_b = 7.61 and 8.29, respectively), the *R*/*S* ratio is only 5.

Molecular modeling studies

In order to understand the binding mode of the enantiomers of (±)-**1** and to explain the low enantioselectivity, docking

Table 2 Affinity constants (pK_i), potency (pD_2) and selectivities of the racemate (±)-**1** and the resolved (*S*)-**1** and (*R*)-**1** enantiomers for human recombinant α_1-adrenoceptor subtypes and 5-HT_{1A} receptors

Compounds (oxalate salts)	pK_i	[^{35}S]GTPγS		pK_i						
	5-HT_{1A}	pD_2	E_{max}	α_{1A}	α_{1B}	α_{1D}	5-HT_{1A}/α_{1d}	α_{1a}/α_{1b}	α_{1d}/α_{1a}	α_{1d}/α_{1b}
(±)-**1**	8.45	8.80	24.4	7.43	7.20	7.93	3	2	3	5
(*S*)-**1**	8.42	6.85	50.0	6.90	6.94	7.84	4	1	9	8
(*R*)-**1**	8.52	7.45	65.3	7.52	7.10	7.64	8	3	1	3
(*R*)-WB 4101	7.39			7.95	7.14	7.98				
(*S*)-WB 4101	8.61			9.39	8.24	9.29				

pK_i and pD_2 values are the mean of 2–3 separate experiments performed in duplicate. Values agreed within 10%.

Table 3 Antagonist potency in pK_b or (pA_2) ± SEM and selectivities of the racemate (±)-**1** and the resolved (*S*)-**1** and (*R*)-**1** enantiomers for α_1-adrenoceptors in isolated rat prostatic vas deferens (α_{1A}), spleen (α_{1B}), and thoracic aorta (α_{1D})

Compounds (oxalate salts)	pK_b or (pA_2) ± SEM					
	α_{1A}	α_{1B}	α_{1D}	α_{1A}/α_{1B}	α_{1D}/α_{1A}	α_{1D}/α_{1B}
(±)-**1**	6.16 ± 0.01	5.86 ± 0.13	(8.20) ± 0.08	0.5	110	219
(*S*)-**1**	6.20 ± 0.03	6.14 ± 0.01	(7.61) ± 0.04	1	26	30
(*R*)-**1**	6.67 ± 0.05	6.51 ± 0.04	(8.29) ± 0.02	1	23	34

pA_2 values were calculated at three different antagonist concentrations. Each concentration was tested at least four times. pK_b values were calculated at one or two concentrations.

studies were performed on the 5-HT_{1A} and α_{1d} receptor models.[15]

To assess if our models are able to stereoselectively discriminate between the two enantiomers of (±)-**1**, the reference 5-HT_{1A} agonist, flesinoxan and one of the most potent and selective α_1-adrenoreceptor antagonists WB 4101 were also docked. These two compounds were chosen on the basis of their high degree of enantioselectivity.[10,12,18] According to our calculations, the binding mode of (*R*)-flesinoxan into the putative 5-HT_{1A} binding site is characterized by a salt bridge interaction between the protonated piperazine nitrogen and the key residue D116 and two H-bond interactions of the hydroxyl group with Y195 and S199 side-chain residues. In addition, the benzamide portion and the benzodioxane moiety display a number of π–π interactions with F19, Y96, W102, F112 and with Y195, W358, F361, F362, respectively (Fig. 4, the *R* enantiomer is depicted in cyan). On the contrary, (*S*)-flesinoxan shows only one H-bond contact with S199, while no salt-bridge and hydrogen bond interactions are detected with the key residue D116 and Y195, respectively (Fig. 4, the *S* enantiomer is depicted in pink). These data are in agreement with the fact that the activity of flesinoxan is due to the (*R*)-enantiomer.[12] Similarly to (*R*)-flesinoxan, (*R*)-**1** displays a salt bridge interaction between the protonated nitrogen atom and the D116 side-chain and an H-bond interaction between the dioxolane oxygen atom and the Y390 residue (Fig. 5, the *R* enantiomer is depicted in yellow). In addition, the phenyl ring interacts with F19, Y96, W102 and F112 residues, while the phenoxy group is widely engaged in π–π stacking interactions with Y195, W358, F361 and F362. As regards the (*S*)-**1** enantiomer, the 1,3-dioxolane core is moderately shifted with respect to (*R*)-**1**, causing the establishment of weaker interactions with the key residues D116 and Y390, thus resulting in a slight decrease of 5-HT_{1A} affinity. On the contrary, the phenyl and phenoxy rings are properly oriented towards F19, Y96, W102, F112 and Y195, W358, F361, F362, respectively, as for (*R*)-**1** (Fig. 5, the *S* enantiomer is depicted in pink). However, the binding mode of (*S*)-**1** is quite similar to that observed for (*R*)-**1**. This is probably due to the flexibility of the two molecules since they contain several freely rotatable bonds. In conclusion, the docking results of the two enantiomers of (±)-**1** into the putative 5-HT_{1A} binding site are in agreement with the poor stereoselectivity observed in the binding experiments.

The docking studies performed on the α_{1d} receptor model showed that (*S*)-WB 4101 is highly stabilized into the putative binding site by a salt-bridge interaction with the D176 side-chain and two H-bond contacts between the oxygen atom of the methoxy group and the oxygen atom of the benzodioxane core with Y254 and K385, respectively (Fig. 6, the *S* enantiomer is depicted in yellow). In addition, several π–π stacking interactions are established between the benzodioxane moiety and the phenoxy ring with W172, F384, F388 and Y254, F364, F365, respectively. On the contrary, (*R*)-WB 4101 displays the same salt-bridge and π–π stacking interactions as (*S*) but only one H-bond contact with K385 (Fig. 6, the *R* enantiomer is

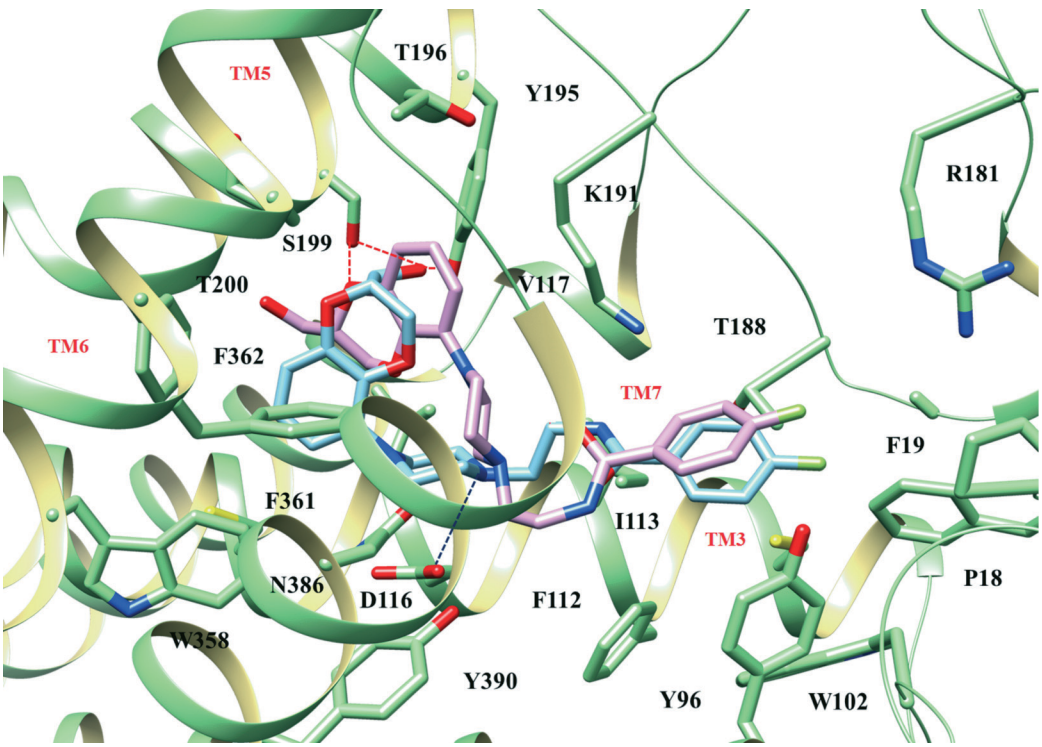

Fig. 4 Selected docking pose of (*R*) and (*S*) flesinoxan into the 5-HT_{1A} putative binding site. The ligands are reported in stick and coloured by atom type (C atom, cyan and pink, respectively). The receptor residues located 5 Å from the two ligands are shown and depicted by atom type (C atom, light green). Hydrogen bond and salt-bridge contacts are reported in red and blue, respectively.

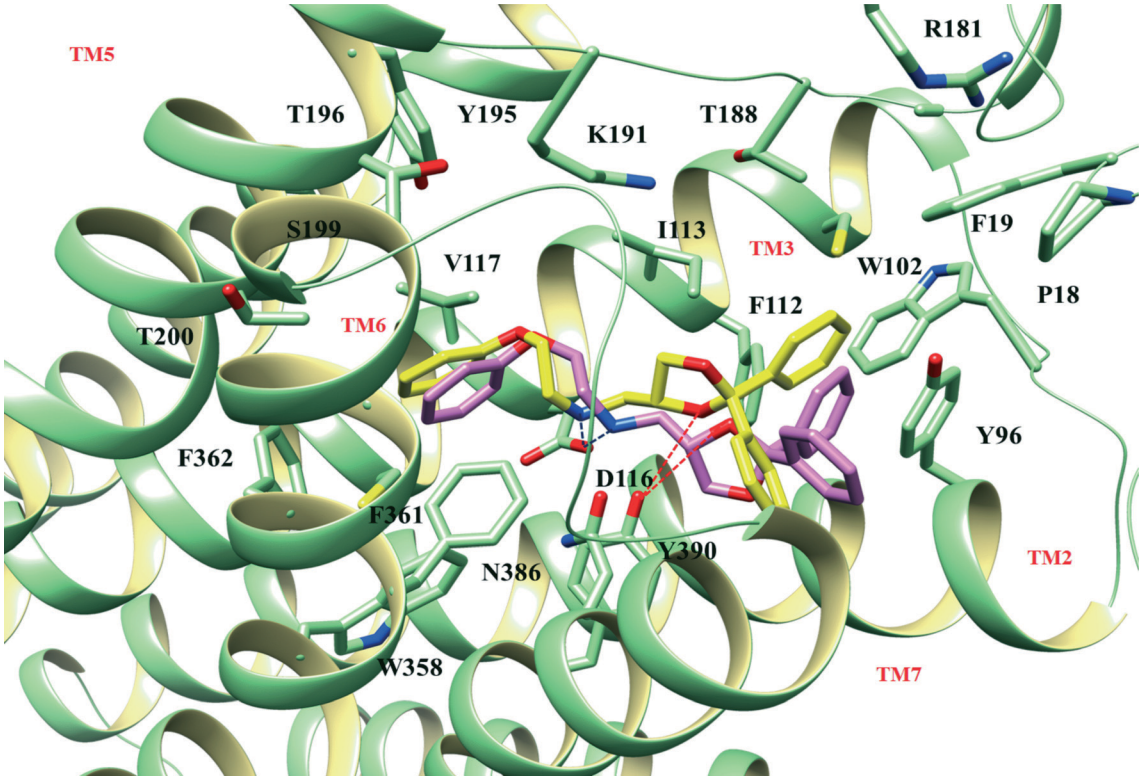

Fig. 5 Selected docking poses of (*R*)-**1** and (*S*)-**1** into the 5-HT_{1A} putative binding site. The two ligands are reported in stick and coloured by atom type (C atom, yellow and pink, respectively). The receptor residues located 5 Å from the ligands are shown and depicted by atom type (C atom, light green). Hydrogen bond and salt-bridge contacts are reported in red and blue, respectively.

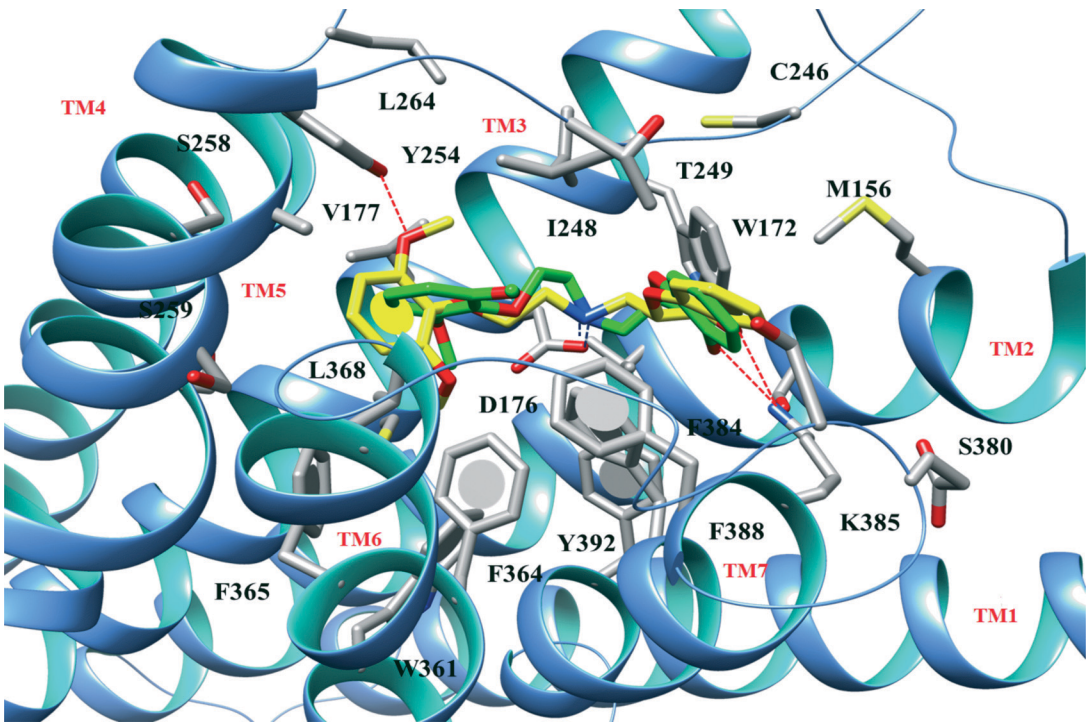

Fig. 6 Selected docking poses of (*R*)- and (*S*)-WB 4101 into the α_{1D} putative binding site. The ligands are reported in stick and coloured by atom type (C atom, green and yellow, respectively). The receptor residues located 5 Å from the agonists are shown and depicted by atom type (C atom, grey). Hydrogen bond and salt-bridge contacts are reported in red and blue, respectively.

depicted in green). The lack of the interaction with Y254 could be an indication of the lower affinity of the (*R*)-enantiomer, in agreement with the binding data (Table 2).

A first comparison between the binding mode of (±)WB 4101 and that of (*S*)-**1** and (*R*)-**1** shows that the replacement of the 1,4-benzodioxane moiety with a 2,2-disubstituted 1,3-dioxolane turns around the docking pose of both enantiomers (Fig. 7). In particular, the phenoxyethylamine chain of (*S*)- and (*R*)-**1** is oriented towards a narrow pocket including M156, W172, F384 and K385, while the 2,2-diphenyl-1,3-dioxolane moiety is projected in a much more deep cavity delimited by V177, Y254, S259, F364, F365 and L368. Thus, the stereogenic centre of (±)-**1** is located in a different cavity with respect to (±)-WB 4101 and this seems to account for the loss of any significant stereo interactions. As a matter of fact, (*S*)-**1** displays a salt bridge with the D176 side-chain, one H-bond between the dioxolane oxygen atom and Y254 residue, and several π–π interactions, while no H-bond contact has been detected with K385 (Fig. 7, the *S* enantiomer is depicted in pink). This might be the reason for the lower affinity of (*S*)-**1** compared to (*S*)-WB 4101 (α_{1d} pK_i = 7.84 and 9.29, respectively). On the other hand, (*R*)-**1** shows a salt-bridge and an H-bond interaction with D176 and K385, respectively, while the dioxolane scaffold is shifted with respect to (*S*)-**1**, guiding the oxygen atom far away from any interaction with Y254 (Fig. 7, the *R* enantiomer is depicted in orange). On the basis of these results, it can be speculated that the low stereoselectivity observed in the binding experiment for (*R*)-**1** and (*S*)-**1** could be due to the fact that both enantiomers share the same type of interaction and none of them is able to H-bond simultaneously with Y254 and K385.

Experimental

Chemistry

Material and methods. All reagents, solvents and other chemicals were used as purchased from Sigma-Aldrich without further purification unless otherwise specified. Solvents used for salification and crystallization of the final compounds were HPLC grade. All synthesized compounds were characterized by NMR, HR-MS and elemental analysis (C, H, N). ^{1}H NMR spectra were recorded with a *Bruker DPX 200* spectrometer operating at 200.13 MHz and a temperature between 270 and 370 K. 2D NMR spectra were recorded on a *Bruker Advance 400 WB* working at frequencies of 400.13 and 100.61 for ^{1}H and ^{13}C, respectively, and at a temperature between 270 and 370 K. Chemical shifts (δ) are reported relative to tetramethylsilane (TMS) as internal standard (s = singlet, brs = broad singlet, d = doublet, dd = double doublet, t = triplet, m = multiplet). ^{1}H–^{1}H correlation spectroscopy (COSY, NOESY), ^{1}H–^{13}C heteronuclear multiple quantum coherence (HMQC) and heteronuclear multiple bond connectivity (HMBC) experiments were performed for determination of ^{1}H–^{1}H and ^{1}H–^{13}C correlations. HR-MS experiments were carried out

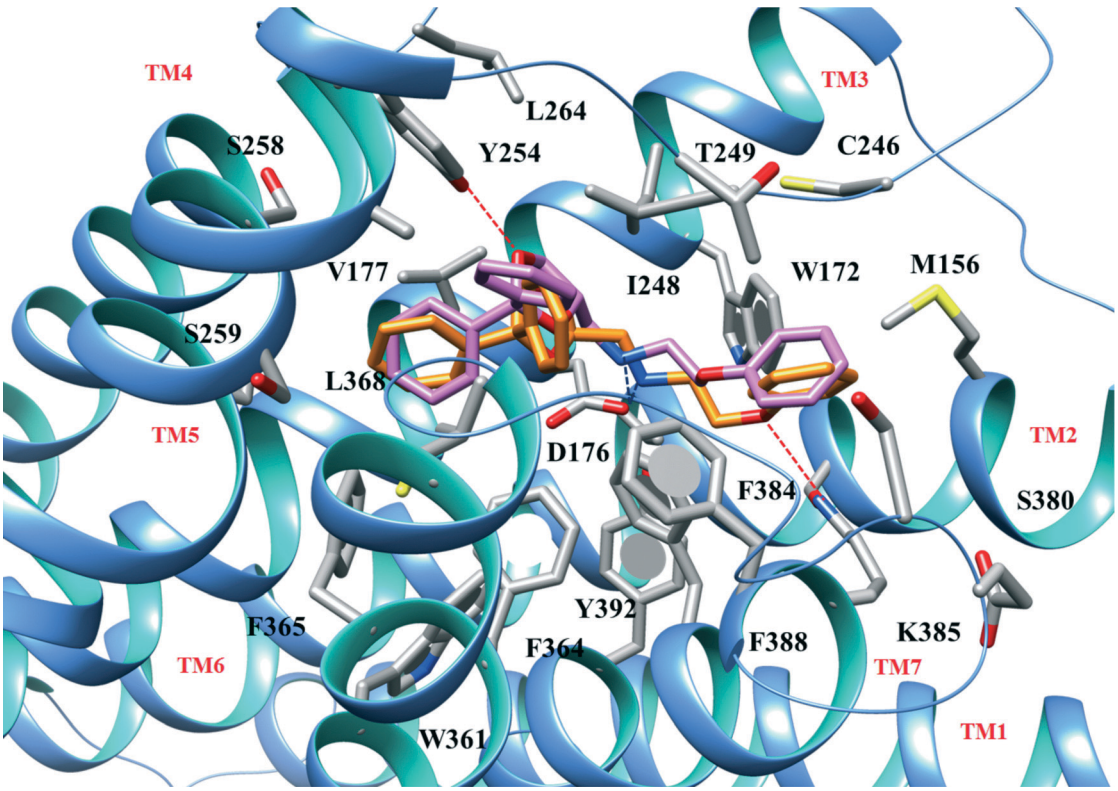

Fig. 7 Selected docking pose of the (*R*)- and (*S*)-**1** enantiomers into the α_{1D} putative binding site. The ligands are reported in stick and coloured by atom type (C atom, orange and pink, respectively). The receptor residues located 5 Å from the agonists are shown and depicted by atom type (C atom, grey). Hydrogen bond and salt-bridge contacts are reported in red and blue, respectively.

using a LC-MS mass spectrometer (*6520 Accurate-Mass Q-TOF LC/MS - Agilent Technologies*) equipped with an ion spray ionization source (ESI). MS (+) spectra were acquired by direct infusion (5 ml min^{-1}) of a solution containing the appropriate sample oxalate salt (10 pmol ml^{-1}), dissolved in 0.1% acetic acid solution, with the mobile phase methanol/water 50 : 50, at the optimum ion voltage of 4800 V. Elemental analysis was performed with an Elemental Analyser 1106 (Carlo Erba Instruments, Italy). Analysis data are reported within ±0.4% of theoretical values. Optical rotations were recorded on a *Perkin Elmer 241* polarimeter at 436 nm and 589 nm. Melting points were determined on a Büchi 510 capillary melting point apparatus and were uncorrected. Reaction progress was monitored by TLC (silica gel 60, F_{254}, Merck). Separations were performed on silica gel columns (Kiesegel 60, 0.040–0.630 mm, Merck) by flash chromatography or by using the Biotage SP1 Purification System. Preparative TLC was carried out on silica gel glass plates (silica gel 60, F_{254}, 2 mm, 20 × 20 cm, Merck).

HPLC analysis of the diastereomers was carried out on a *1100 System* (Agilent Technologies) consisting of a vacuum degasser, a quaternary pump, an autosampler, a thermostated column compartment and a diode array detector, using a Speri-5 silica gel column (250 × 4.6 i.d. mm, 5 μm, Applied Biosystems), with a mobile phase cyclohexane/ethyl acetate 70 : 30 (v/v), at a flow rate of 1.0 mL min^{-1}. The column was thermostated at 20 °C. The sample injection volume was 5 μL. The detection wavelength was set at 254 nm. The total analysis time was 20 min.

Compound names were generated with MarvinSketch software, version 5.10.1.

[(2,2-diphenyl-1,3-dioxolan-4-yl)methyl](2-phenoxyethyl)amine (1). The compound was synthesized as previously reported.[7] 1.45 g (3.87 mmol), yield 75%, ^{1}H-NMR (200 MHz, $CDCl_3$): δ = 1.67 (brs, 1H, NH), 2.83 (dd, *J* = 12.3, 4.8 Hz, 1H, CHa–NH), 2.93 (dd, *J* = 12.3, 6.8 Hz, 1H, CHb–NH), 3.03 (t, *J* = 5.3 Hz, 2H, *CH*$_2$–CH$_2$–O–Ph), 3.84 (dd, *J* = 7.9, 6.3 Hz, 1H, H5a-dioxolane), 4.06 (t, *J* = 5.3 Hz, 2H, CH$_2$–*CH*$_2$–O–Ph), 4.09 (dd, *J* = 7.9, 7.0 Hz, 1H, H5b-dioxolane), 4.37 (m, 1H, H4-dioxolane), 6.90 (m, 2H, H2/H6-phenoxy), 6.95 (m, 1H, H4-phenoxy), 7.24–7.38 (m, 8H, H3/H5-phenoxy, H2/H6-diphenyl, H4-diphenyl), 7.47–7.56 (m, 4H, H3/H5-diphenyl).

The free amine was transformed into the corresponding oxalate salt which was crystallized from methanol to give compound (**1**), m.p. 189°–191 °C; ^{1}H-NMR (200 MHz, DMSO): δ = 3.03 (dd, *J* = 12.0, 7.7 Hz, 1H, CHa–NH), 3.15 (dd, *J* = 12.0, 3.9 Hz, 1H, CHb–NH), 3.28 (t, *J* = 5.1 Hz, 2H, *CH*$_2$–CH$_2$–O–Ph), 3.95 (dd, *J* = 8.0, 6.3 Hz, 1H, H5a-dioxolane), 4.20 (dd, *J* = 8.0, 6.8 Hz, 1H, H5b-dioxolane), 4.17 (t, *J* = 5.1 Hz, 2H, CH$_2$–*CH*$_2$–O–Ph), 4.40 (m, 1H, H4-dioxolane), 6.92–6.99 (m, 3H, H2/H6-phenoxy, H4-phenoxy), 7.26–7.46 (m, 12H, H3/H5-phenoxy, H2/H6-diphenyl, H4-diphenyl, H3/H5-diphenyl).

Anal. calcd. for $C_{26}H_{27}O_7N$: C, 67.09; H, 5.85; N, 3.01. Found: C, 67.35; H, 5.81; N, 3.11. HR-MS (ESI-Q-Tof): calc. for $C_{24}H_{25}O_3N$ $[M + H]^+$ 375.1834; found 375.1839, Dev. 1.3 ppm.

(2*S*)-1-(4-methylbenzenesulfonyl)pyrrolidine-2-carbonyl chloride (*S*)-3. To a solution of (*S*)-proline (1 g, 8.7 mmol) in 7.5 ml of water was added Na_2CO_3 (1.70 g, 16.0 mmol) and then slowly *p*-toluenesulfonyl chloride (2.00 g, 10.5 mmol) at 0 °C. The reaction mixture was stirred at room temperature for 22 h. 1 N HCl was added until the solution was acidic and the resulting mixture was taken up in ethyl acetate (4 × 15 ml). The organic phase was dried over Na_2SO_4, filtered, and the solvent evaporated. 1.82 g (6.8 mmol, 78% yield) of *N*-tosyl-(*S*)-proline was obtained and used for the next step without any further purification. *N*-tosyl-(*S*)-proline (1 g, 3.5 mmol) was dissolved in 6 ml of toluene; to this solution was carefully added thionyl chloride (1.32 g, 11.1 mmol). The reaction mixture was refluxed for 30 min. After removal of the solvent, 1.07 g (3.7 mmol, 98% yield) of (*S*)-**3** was obtained and immediately allowed to react in the next step without any further purification.[19] M.p. 56–57 °C; ^{1}H-NMR (400 MHz, $CDCl_3$): δ = 1.84–1.90 (m, 1H, CHa-4 proline), 1.92–2.05 (m, CHb-4, CHa-3 proline), 2.15–2.23 (m, 1H, CHb-3 proline), 2.48 (s, 3H, CH_3 tosyl), 3.35–3.45 (m, 1H, CHa-5 proline), 3.50–3.56 (m, 1H, CHb-5 proline), 4.65 (dd, *J* = 6.1, 7.9 Hz, 1H, CH-2 proline), 7.37 (d, *J* = 8.0 Hz, 2H, CH-3, CH-5 arom. tosyl), 7.78 ppm (d, *J* = 8.0 Hz, 2H, CH-2, CH-6 arom. tosyl).

(2*S*)-*N*-[(2,2-diphenyl-1,3-dioxolan-4-yl)methyl]-1-(4-methylbenzenesulfonyl)-*N*-(2-phenoxyethyl)pyrrolidine-2-carboxamide (2). To a solution of (±)-**1** in CH_2Cl_2 was added pyridine and a solution of **3** in CH_2Cl_2 at 0 °C. The reaction mixture was warmed to RT and refluxed for 50 min. $NaHCO_3$ was added, and the organic layer was separated and washed with H_2O, dried over Na_2SO_4 and concentrated under reduced pressure. The residue was purified by flash chromatography (cyclohexane/EtOAc 80 : 20) or preparative TLC (cyclohexane/EtOAc 50 : 50) to yield the single diastereomer.

(2*S*)-*N*-{[(4*S*)-2,2-diphenyl-1,3-dioxolan-4-yl]methyl}-1-(4-methylbenzenesulfonyl)-*N*-(2-phenoxyethyl)pyrrolidine-2-carboxamide (2*S*,4*S*)-2. 0.38 g (0.6 mmol) of (*S*,*S*)-**4**, 21% yield.

(*Z*) conformer (56%).

^{1}H-NMR (400 MHz) ($CDCl_3$): δ = 1.74–1.88 (m, 1H, H4a proline), 1.93–2.08 (m, 1H, H3a proline), 2.08–2.20 (m, 2H, H4b proline, H3b proline), 2.42 (s, 3H, CH3 tosyl), 3.30 (dd, *J* = 14.0, 7.5 Hz, 1H, CH2–N), 3.4–3.54 (m, 2H, H5 proline), 3,74 (m, 1H, N–CH2), 3.83 (dd, *J* = 8.2, 6.9 Hz, 1H, H5a-dioxolane), 4.03 (dd, *J* = 14.0, 3.6 Hz, 1H, CH2–N), 4,11 (m, 1H, H5b-dioxolane), 4.32 (t, *J* = 4.5, 2H, CH2O–Ph), 4.35 (dd, *J* = 9.9, 4.1 Hz, 1H, N–CH2), 4.42 (m, 1H, H4 dioxolane), 5.05 (dd, *J* = 3.7, *J* = 7.7, 1H, H2 proline), 6.92 (m, 2H, H2/H6-phenoxy), 7.03 (m, 1H, H4-phenoxy), 7.26 (d, *J* = 8.2 Hz, 2H, H3/H5-tosyl), 7.26–7.39 (m, 8H, H3/H5-phenoxy, H2/H6 and H4-phenyl), 7.42–7.54 (m, 4H H3/H5-phenyl), 7.75 (d, *J* = 8.2 Hz, 2H, H2/H6-tosyl).

^{13}C-NMR (100 MHz) ($CDCl_3$): δ = 21.55 (CH3-Tosyl), 24.88 (C4-proline), 31.42 (C3-proline), 48.65 (C5-proline), 49.0 (CH2–CH2–O–Ph), 50.46 (CH2–N–CO), 57.53 (C2-proline), 65.83 (CH2–CH2–O–Ph), 67.88 (C5-dioxolane), 75.67 (C4-dioxolane), 110.71 (C2-dioxolane), 114.51 (C2-phenoxy), 121.33 (C4-phenoxy), 126.12 (C4-phenyl), 127.45 (C2-tosyl), 128.16 (C2-phenyl), 129.50

(C3-phenoxy), 129.55 (C3-phenyl), 129.63 (C3-tosyl), 136.16 (C1-tosyl), 143.58 (C4-tosyl), 158.36 (C1-phenoxy), 172.91 (CO–N).

(*E*) conformer (44%).

^{1}H-NMR (400 MHz, CDCl3): δ = 1.47–1.58 (m, 2H, H3a proline, H4a proline), 1.74–1.92 (m, 1H, H3b proline), 1.97–2.01 (m, 1H, H4b proline), 2.42 (s, 3H, CH3 tosyl), 3.4–3.54 (m, 2H, H5 proline), 3.58 (dd, *J* = 15.3, 3.4 Hz, 1H, CH2–N), 3.70–3.86 (m, 2H, N–CH2), 4.02 (m, 1H, H5a-dioxolane), 4.13 (m, 1H, H5b-dioxolane), 4.19 (t, 4.9 Hz, 2H, CH2O–Ph), 4.21 (dd, *J* = 15.3, 8.9, 1H, CH2–N), 4.59 (m, 1H, H4 dioxolane), 4.83 (dd, *J* = 4.1, 7.8 Hz, 1H, H2-proline), 6.86 (m, 2H, H2/H6-phenoxy), 6.99 (m, 1H, H4-phenoxy), 7.23 (d, *J* = 8.2 Hz, 2H, H3/H5-tosyl), 7.27–7.38 (m, 8H, H3/H5-phenoxy, H2/H6 and H4-phenyl), 7.42–7.55 (m, 4H, H3/H5-phenyl), 7.72 (d, J 8.2 Hz, 2H, H2/H6-tosyl).

^{13}C-NMR (100 MHz) ($CDCl_3$): δ = 21.55 (CH3-tosyl), 24.90 (C4-proline), 31.52 (C3-proline), 48.56 (C5-proline), 49.0 (CH2–CH2–O–Ph), 50.46 (CH2–N–CO), 57.43 (C2-proline), 65.83 (CH2–CH2–O–Ph), 68.08 (C5-dioxolane), 75.70 (C4-dioxolane), 109.99 (C2-dioxolane), 114.54 (C2-phenoxy), 121.05 (C4-phenoxy), 126.17 (C4-phenyl), 127.32 (C2-tosyl), 128.14 (C2-phenyl), 129.50 (C3-phenoxy), 129.58 (C3-phenyl), 129.63 (C3-tosyl), 136.16 (C1-tosyl), 143.58 (C4-tosyl), 158.36 (C1-phenoxy), 172.87 (CO–N).

(2*S*)-*N*-{[(4*R*)-2,2-diphenyl-1,3-dioxolan-4-yl]methyl}-1-(4-methylbenzenesulfonyl)-*N*-(2-phenoxyethyl)pyrrolidine-2-carboxamide (2*S*,4*R*)-2. 0.45 g (0.7 mmol) of (*S*,*R*)-**4**, 24% yield.

(*Z*) conformer (77%).

^{1}H-NMR (400 MHz) ($CDCl_3$): δ = 1.80–1.91 (m, 1H, H4a proline), 1.92–1.98 (m, 1H, H3a proline), 2.03–2.20 (m, 2H, H4b proline, H3b proline), 2.40 (s, 3H, CH3 tosyl), 3.40 (dd, *J* = 14.0, 7.5 Hz, 1H, CH2–N), 3.42–3.54 (m, 2H, H5 proline), 3,80–3.91 (m, 1H, N–CH2), 3.81 (dd, *J* = 8.3, 6.9 Hz, 1H, H5a-dioxolane), 3.94 (dd, *J* = 14.0, 7.5 Hz, 1H, CH2–N), 4,08 (dd, *J* = 8.3, 6.9 Hz, 1H, H5b-dioxolane), 4.16 (t, *J* = 5.2, 2H, CH2O–Ph), 4.23–4.31 (m, 1H, N–CH2), 4.42 (m, 1H, H4 dioxolane), 5.05 (dd, *J* = 3.7, *J* = 7.9, 1H, H2 proline), 6.91 (m, 2H, H2/H6-phenoxy), 7.02 (m, 1H, H4-phenoxy), 7.17 (d, *J* = 8.0 Hz, 2H, H3/H5-tosyl), 7.27–7.41 (m, 8H, H3/H5-phenoxy, H2/H6 and H4-phenyl), 7.51–7.59 (m, 4H, H3/H5-phenyl), 7.74 (d, *J* 8.25 Hz, 2H, H2/H6-tosyl).

^{13}C-NMR (100 MHz) ($CDCl_3$): δ = 21.51 (CH3-tosyl), 24.92 (C4-proline), 31.46 (C3-proline), 48.46 (C5-proline), 49.18 (CH2–CH2–O–Ph), 50.46 (CH2–N–CO), 57.47 (C2-proline), 65.64 (CH2–CH2–O–Ph), 68.01 (C5-dioxolane), 76.21 (C4-dioxolane), 109.96 (C2-dioxolane), 114.46 (C2/C6-phenoxy), 121.36 (C4-phenoxy), 126.06 (C3/C5-phenyl), 127.36 (C2-tosyl), 128.08 (C2/C6-phenyl), 128.30 (C4-phenyl), 129.52 (C3-tosyl), 129.65 (C3/C5-phenoxy), 136.36 (C1-tosyl), 143.24 (C4-tosyl), 158.31 (C1-phenoxy), 173.08 (CO–N).

(*E*) conformer (23%).

^{1}H-NMR (400 MHz) ($CDCl_3$): δ = 1.77–1.91 (m, 2H, H3a proline, H4a proline), 1.92–2.0 (m, 1H, H3b proline), 2.03–2.20 (m, 1H, H4b proline), 2.41 (s, 3H, CH3 tosyl), 3.42–3.54 (m, 2H, H5 proline), 3.75 (dd, *J* = 15.7, 6.9 Hz, 1H, CH2–N), 3.80–3.91 (m, 2H, N–CH2), 3.92 (m, 1H, H5a-dioxolane), 4.04 (dd, *J* = 15.7, 4.0 Hz, 1H, CH2–N), 4.07 (m, 2H, CH2O–Ph),4.22 (m, 1H, H5b dioxolane), 4.50 (m, 1H, H4-dioxolane),4.84 (dd, *J* = 4.0, 8.0 Hz, 1H, H2-proline), 6.86 (m, 2H, H2/H6-phenoxy), 6.99 (m, 1H, H4-phenoxy), 7.19 (d, *J* = 8.0 Hz, 2H, H3/H5-tosyl), 7.27–7.41 (m, 8H, H3/H5-phenoxy, H2/H6 and H4-phenyl), 7.51–7.59 (m, 4H, H3/H5-phenyl), 7.72 (d, *J* 8.0 Hz, 2H, H2/H6-tosyl).

^{13}C-NMR (100 MHz) ($CDCl_3$): δ = 21.55 (CH3-tosyl), 24.86 (C4-proline), 31.11 (C3-proline), 48.43 (C5-proline), 49.21 (CH2–CH2–O–Ph), 50.46 (CH2–N–CO), 57.51 (C2-proline), 65.65 (CH2–CH2–O–Ph), 67.90 (C5-dioxolane), 76.30 (C4-dioxolane), 110.02 (C2-dioxolane), 114.50 (C2/C6-phenoxy), 121.01 (C4-phenoxy), 125.90 (C3/C5-phenyl), 127.36 (C2-tosyl), 128.08 (C2/C6-phenyl), 128.30 (C4-phenyl), 129.52 (C3-tosyl), 129.65 (C3/C5-phenoxy), 136.36 (C1-tosyl), 143.22 (C4-tosyl), 158.31 (C1-phenoxy), 173.08 (CO–N).

{[(4*S*)-2,2-diphenyl-1,3-dioxolan-4-yl]methyl} (2-phenoxyethyl)amine (*S*)-1. (2*S*,4*S*)-**2** was added to a 2 N solution of freshly prepared sodium ethoxide. The mixture was heated under reflux for 2 h. The solvent was evaporated and the residue was dissolved in H_2O and extracted three times with $CHCl_3$. The organic phase was washed with brine, dried over Na_2SO_4 and the solvent removed under vacuum. The product was isolated without any further purification. 0.06 g (0.2 mmol) of (*S*)-**1**, 90% yield.

^{1}H-NMR (400 MHz, $CDCl_3$): δ = 2.09 (brs, 1H, NH), 2.89 (dd, *J* = 12.3, 4.5 Hz, 1H, CHa–NH), 2.97 (dd, *J* = 12.3, 7.1 Hz, 1H, CHb–NH), 3.09 (t, *J* = 5.1 Hz, 2H, CH_2–CH_2–O–Ph), 3.91 (dd, *J* = 8.0, 6.2 Hz, 1H, H5a-dioxolane), 4.11 (t, *J* = 5.1 Hz, 2H, CH_2–CH_2–O–Ph), 4.14 (dd, *J* = 8.0, 7.0 Hz, 1H, H5b-dioxolane), 4.42 (m, 1H, H4-dioxolane), 6.95 (m, 2H, H2/H6-phenoxy), 7.00 (m, 1H, H4-phenoxy), 7.29–7.40 (m, 8H, H3/H5-phenoxy, H2/H6-diphenyl, H4-diphenyl), 7.51–7.60 (m, 4H, H3/H5-diphenyl).

^{13}C-NMR (100 MHz, $CDCl_3$): δ = 48.95 (CH_2–CH_2–O–Ph), 52.36 (1C, CH_2–NH), 67.07 (CH_2–CH_2–O–Ph), 68.19 (C5-dioxolane), 76.17 (C4-dioxolane), 109.97 (C2-dioxolane), 114.60 (C2/C6-phenoxy), 120.91 (C4-phenoxy), 126.16 (C3/C5-diphenyl), 128.06 (C4-diphenyl), 128.10 (C2/C6-diphenyl), 129.19 (C3/C5-phenoxy), 142.28 (C1-diphenyl), 158.80 (C1-phenoxy). $[\alpha]_D$ = +9.6° (0.01 g ml^{-1} in $CHC1_3$).

The free amine (*S*)-**1** (0.26 g, 0.70 mmol) was dissolved in diethyl ether and treated with 1.0 eq. of oxalic acid to give the corresponding oxalate salt which was crystallized from methanol to give: 0.09 g (0.2 mmol), 43% yield; mp: 190°–192 °C.

^{1}H-NMR (400 MHz, DMSO): δ = 3.13 (dd, *J* = 12.7, 7.9 Hz, 1H, CHa–NH), 3.25 (dd, *J* = 12.7, 3.6 Hz , 1H, CHb–NH), 3.38 (m, 2H, CH_2–CH_2–O–Ph), 3.85 (dd, *J* = 8.1, 6.7 Hz, 1H, C5a-dioxolane), 4.09 (dd, *J* = 8.1, 7.1 Hz, 1H, C5a-dioxolane), 4.23 (t, *J* = 4.5 Hz, 2H, CH_2–CH_2–O–Ph), 4.47 (m, 1H, H4-dioxolane), 6.93–7.03 (m, 3H, H2/H6-phenoxy, H4-phenoxy), 7.27–7.43 (m, 8H, H3/H5-phenoxy, H2/H6-diphenyl, H4-diphenyl), 7.43–7.50 (m, 4H, H3/H5-diphenyl).

^{13}C-NMR (100 MHz, DMSO): δ = 47.17 (CH_2–CH_2–O–Ph), 50.17 (1C, CH2–NH), 64.25 (CH_2–CH_2–O–Ph), 67.97 (C5-dioxolane), 73.38 (C4-dioxolane), 110.25 (C2-dioxolane), 115.08 (2C, C2/C6-phenoxy), 121.60 (C4-phenoxy), 126.35 (4C, C3/C5-diphenyl), 128.67 (2C, C4-diphenyl), 128.70 (4C, C2/C6-diphenyl), 130.03 (2C, C3/C5-phenoxy), 142.34 (C1-diphenyl), 158.33 (C1-phenoxy).

Anal. calcd. for $C_{26}H_{27}NO_7$: C, 67.09; H, 5.85; N, 3.01. Found: C, 67.29; H, 5.87; N, 3.10.

HR-MS (ESI-Q-Tof): calc. for $C_{24}H_{25}NO_3$ $[M + H]^+$ 375.1834; found 375.1827, dev. 1.9 ppm.

{[(4*R*)-2,2-diphenyl-1,3-dioxolan-4-yl]methyl} (2-phenoxyethyl)amine (*R*)-1. The compound was synthesized from (*S*,*R*)-2 following the procedure described for (*S*)-**1**; 0.06 g (0.2 mmol) of (*R*)-**1**, 89% yield.

^{1}H-NMR (400 MHz, $CDCl_3$) identical to that of (*S*)-**1**; $[\alpha]_D$ = −9.2° (0.01 g ml^{-1} in $CHC1_3$).

The free amine (*R*)-**1** (0.16 g, 0.40 mmol) was dissolved in diethyl ether and treated with 1.0 eq. of oxalic acid to give the corresponding oxalate salt which was crystallized from methanol to give: 0.05 g (0.1 mmol), 38% yield; mp 189–191 °C; ^{1}H NMR (400 MHz, DMSO) identical to that of (*S*)-**1**.

Anal. calcd. for $C_{26}H_{27}NO_7$: C, 67.09; H, 5.85; N, 3.01. Found: C, 67.35; H, 5.81; N, 3.11.

HR-MS (ESI-Q-Tof): calc. for $C_{24}H_{25}NO_3$ $[M + H]^+$ 375.1834; found 375.1839, dev. 1.3 ppm.

(4*R*)-4-(chloromethyl)-2,2-diphenyl-1,3-dioxolane (*R*)-4. The compound was synthesized as previously reported starting from (2*R*)-(+)-3-chloro-1,2-propanediol.[7] 0.67 g (2.4 mmol) of (4*R*)-**4**, 82% yield.

^{1}H-NMR (200 MHz, $CDCl_3$): δ = 3.48 (dd, J = 10.9, 7.9 Hz, 1H, CHa–Cl); 3.69 (dd, J = 10.9, 4.8 Hz, 1H, CHb–Cl); 4.02 (dd, J = 8.5, 5.2 Hz, 1H, H5a-dioxolane); 4.14 (dd, J = 8.5, 6.5 Hz, 1H, H5b-dioxolane); 4.44 (m, 1H, H4-dioxolane); 7.25–7.39 (m, 6H, H2/H6-diphenyl, H4-diphenyl); 7.46–7.57 (m, 4H, H3/H5-diphenyl). $[\alpha]_D$ = +37.3° (0.01 g ml^{-1} in CH_2C1_2).

(4*S*)-4-(chloromethyl)-2,2-diphenyl-1,3-dioxolane (*S*)-4. The compound was synthesized as previously reported starting from (*S*)-(−)-3-chloro-1,2-propanediol.[7] 0.67 g (2.4 mmol) of (4*S*)-**4**, 82% yield.

^{1}H-NMR (200 MHz, $CDCl_3$) identical to that of (*R*)-**4**; $[\alpha]_D$ = −37.8° (0.01 g ml^{-1} in CH_2C1_2).

{[(4*S*)-2,2-diphenyl-1,3-dioxolan-4-yl]methyl}(2-phenoxyethyl)-amine (*S*)-5. The compound was synthesized from (*R*)-**4** as previously reported.[7] 0.52 g (1.4 mmol), 58% yield. ^{1}H-NMR (400 MHz, $CDCl_3$) and ^{13}C-NMR (100 MHz, $CDCl_3$) identical to those of (*S*)-**1**; $[\alpha]_D$ = +9.4° (0.011 g ml^{-1} in $CHC1_3$).

The free amine (0.16 g, 0.4 mmol) was dissolved in diethyl ether and treated with 1.0 eq. of oxalic acid to give the corresponding oxalate salt which was crystallized from methanol to give: 0.09 g (0.19 mmol), 45% yield; mp 190–192 °C; ^{1}H NMR (400 MHz, DMSO) and ^{13}C-NMR (100 MHz, DMSO) identical to those of (*S*)-**1**.

Anal. calcd. for $C_{24}H_{25}NO_3$: C, 76.77; H, 6.71; N, 3.73. Found: C, 76.71; H, 6.72; N, 3.69. HRMS-ESI: calc. for $C_{24}H_{26}NO_3$ [M + H] + 376.2383; found 376.2382.

{[(4*R*)-2,2-diphenyl-1,3-dioxolan-4-yl]methyl}(2-phenoxyethyl)-amine (*R*)-5. The compound was synthesized from (*S*)-**4** as previously reported.[7] 0.58 g (1.6 mmol), 64% yield; $[\alpha]_D$ = −9.1° (0.011 g ml^{-1} in $CHC1_3$).

^{1}H-NMR (400 MHz, DMSO) and ^{13}C-NMR (100 MHz, $CDCl_3$) identical to those of (*S*)-**5**.

The free amine (0.16 g, 0.40 mmol) was dissolved in diethyl ether and treated with 1.0 eq. of oxalic acid to give the corresponding oxalate salt which was crystallized from methanol to give: 0.05 g (0.1 mmol), 38% yield; mp 189–191 °C; ^{1}H NMR (400 MHz, DMSO) and ^{13}C-NMR (100 MHz, DMSO) identical to those of (*S*)-**5**.

Anal. calcd. for $C_{24}H_{25}NO_3$: C, 76.77; H, 6.71; N, 3.73. Found: C, 76.84; H, 6.76; N, 3.75. HRMS-ESI: calc. for $C_{24}H_{26}NO_3$ [M + H] + 376.2383; found 376.2385.

Pharmacology

The compounds were tested as oxalate salts. The purity of the salts was confirmed by elemental analysis and the values obtained are within ±0.4% of the calculated ones. The exact mass of the salts was confirmed by HPLC-QTOF measurement. The HPLC-UV purity was found to be >98%. All experiments were performed in compliance with the relevant laws and institutional guidelines.

Functional antagonism in isolated tissues

Male Wistar rats (275–300 g) were killed by cervical dislocation, and the organs required were isolated, freed from adhering connective tissues, and set up rapidly under a suitable resting tension in 20 mL of organ baths containing physiological salt solution kept at 37 °C and aerated with 5% CO_2–95% O_2 at pH 7.4. Concentration–response curves were constructed by cumulative addition of the agonist. The concentration of the agonist in the organ bath was increased approximately 3-fold at each step, with each addition being made only after the response to the previous addition had attained a maximal level and remained steady. Contractions were recorded by means of a force displacement transducer connected to the Mac Lab system PowerLab/800 and to a polygraph channel recorder (Gemini). In addition, parallel experiments in which tissues did not receive any antagonist were run in order to check any variation in sensitivity.

Vas deferens prostatic portion

This tissue was used to assess the antagonism toward α_{1A} adrenoceptors.[20] Prostatic portions of 2 cm length were mounted under 0.5 g of tension at 37 °C in Tyrode's solution of the following composition (mM): NaCl, 130; KCl, 1; $CaCl_2$, 1.8; $MgCl_2$, 0.89; NaH_2PO_4, 0.42; $NaHCO_3$, 25; glucose, 5.6. cocaine hydrochloride (0.1 μM), to prevent the neuronal uptake of (−)-noradrenaline. The preparations were equilibrated for 60 min by washing every 15 min. After the equilibration period, tissues were primed twice by addition of 10 μM noradrenaline. After another washing and equilibration period of 60 min, a noradrenaline concentration–response curve was constructed (basal response). The antagonist was equilibrated for 30 min before construction of a new concentration–response curve to the agonist. (−)-Noradrenaline solutions contained 0.05% $Na_2S_2O_5$ to prevent oxidation.

Spleen

This tissue was used to assess the antagonism toward α_{1B} adrenoceptors.[21] The spleen was removed and bisected longitudinally into two strips, which were suspended in tissue baths containing Krebs solution of the following composition (mM): NaCl, 120; KCl, 4.7; $CaCl_2$, 2.5; $MgSO_4$, 1.5; KH_2PO_4, 1.2; $NaHCO_3$, glucose, 11; K_2EDTA, 0.01. Propranolol hydrochloride (4 μM) was added to block β-adrenoceptors. The spleen strips were placed under 1 g of resting tension and equilibrated for 2 h. The cumulative concentration–response curves to phenylephrine were measured isometrically and obtained at 30 min intervals, the first one being discarded and the second taken as a control. The antagonist was allowed to equilibrate for 30 min before constructing a new concentration–response curve to the agonist.

Aorta

This tissue was used to assess the antagonism toward α_{1D} adrenoceptors.[22] Thoracic aorta was cleaned from extraneous connective tissues and placed in Krebs solution of the following composition (mM): NaCl, 118.4; KCl, 4.7; $CaCl_2$, 1.9; $MgSO_4$, 1.2; NaH_2PO_4, 1.2; $NaHCO_3$, 25; glucose, 11.7; K_2EDTA, 0.01. Cocaine hydrochloride (0.1 μM) and propranolol hydrochloride (4 μM) were added to prevent the neuronal uptake of (−)-noradrenaline and to block β-adrenoceptors, respectively. Two helicoidal strips (15 mm × 3 mm) were cut from each aorta, beginning from the end that is most proximal to the heart. The endothelium was removed by rubbing with filter paper. The absence of acetylcholine (100 μM) induced relaxation in preparations contracted with (−)-noradrenaline (1 μM) was taken as an indicator that the vessels were denuded successfully. Vascular strips were then tied with surgical thread and suspended in a jacketed tissue bath containing Tyrode's solution. Strip contractions were measured isometrically. After at least a 2 h equilibration period under an optimal tension of 1 g, cumulative (−)-noradrenaline concentration–response curves were recorded at 1 h intervals, the first two being discarded and the third one taken as control. The antagonist was equilibrated with the tissue for 30 min before the generation of the fourth cumulative concentration–response curve to (−)-noradrenaline. (−)-Noradrenaline solutions contained 0.05% K_2EDTA in 0.9% NaCl to prevent oxidation.

Radioligand binding assay at human recombinant 5-HT_{1A} receptors and α_1 adrenoceptor subtypes

A human cell line (HeLa) stably transfected with genomic clone G-21 coding for the human 5-HT_{1A} serotoninergic receptor was used. Cells were grown as monolayers in Dulbecco's modified Eagle's medium supplemented with 10% fetal calf serum and gentamycin (100 μg mL^{-1}) under 5% CO2 at 37 °C. Cells were detached from the growth flask at 95% confluence by a cell scraper and were lysed in ice-cold Tris (5 mM) and EDTA buffer (5 mM, pH 7.4). Homogenates were centrifuged for 20 min at 40 000 *g*, and pellets were resuspended in a small volume of ice-cold Tris/EDTA buffer (above) and immediately frozen and stored at 70 °C until use. On the day of the experiment, cell membranes (80–90 μg of protein) were resuspended in binding buffer (50 mM Tris, 2.5 mM $MgCl_2$, and 10 mM pargyline, pH 7.4). Membranes were incubated in a final volume of 0.32 mL for 30 min at 30 °C with 1 nM [^{3}H]8-OH-DPAT, in the absence or presence of various concentrations of the competing drugs (1 pM to 1 μM); each experimental condition was performed in triplicate. Nonspecific binding was determined in the presence of 10 μM 5-HT. Binding to recombinant human α_1 adrenoceptor subtypes was performed in membranes from Chinese hamster ovary (CHO) cells transfected by electroporation with DNA expressing the gene encoding each α_1 adrenoceptor subtype. Cloning and stable expression of the human α_1 adrenoceptor genes were performed as described.[23] CHO cell membranes (70 μg of protein) were incubated in 50 mM Tris (pH 7.4) with 0.1–0.4 nM [^{3}H]prazosin, in a final volume of 0.32 mL for 30 min at 25 °C, in the absence or presence of competing drugs (1 pM to 1 μM). Nonspecific binding was determined in the presence of 10 μM Tamsulosin. The incubation was stopped by addition of ice-cold Tris buffer and rapid filtration through Unifilter B filters (Perkin-Elmer) using a Filtermate cell harvester (Packard), and the radioactivity retained on the filters was determined by TopCount, Perkin-Elmer liquid scintillation counting at 90% efficiency.

[^{35}S]GTPγS binding assay

The effects of the various compounds tested on [^{35}S]GTPγS binding in HeLa cells expressing the recombinant human 5-HT_{1A} receptor were evaluated according to the method of Stanton and Beer[24] with minor modifications. Stimulation experiments: cell membranes (50–70 μg of protein) were resuspended in a buffer containing 20 mM HEPES, 3 mM $MgSO_4$, and 120 mM NaCl (pH 7.4). The membranes were incubated with 30 μM GDP and various concentrations (from 0.1 nM to 10 μM) of test drugs or 8-OH-DPAT (reference curve) for 20 min at 30 °C in a final volume of 0.5 mL. Samples were transferred to ice, [^{35}S]GTPγS (200 pM) was added, and samples were incubated for another 30 min at 30 °C. The pre-incubation with both agonist and antagonist, before initiating the [^{35}S]GTPγS binding, ensures that the agonist and antagonist are at equilibrium. Nonspecific binding was determined in the presence of 10 μM GTPγS. Incubation was stopped by the addition of ice-cold HEPES buffer and rapid filtration on Unifilter B filters (Perkin Elmer) using a Filtermate cell harvester (Packard). The filters were washed with ice-cold Hepes buffer, and the radioactivity retained on the filters was determined by TopCount, Perkin Elmer liquid scintillation counting at 90% efficiency.

Data analysis

Binding data were analyzed using the nonlinear curve-fitting program GraphPad (Prism for Windows, version 5.04). Scatchard plots were linear for all preparations. None of the pseudo-Hill coefficients (nH) were significantly different from unity ($p > 0.05$). Equilibrium dissociation constants (K_i) were

derived from the Cheng–Prusoff equation $K_i = IC_{50}/(L/K_d)$, where L and K_d are the concentration and the equilibrium dissociation constant of the radioligand. pK_i values are the mean of 2–3 separate experiments performed in duplicate.[25] Stimulation of [^{35}S]GTPγS binding induced by the compounds tested was expressed as the percent increase in binding above the basal value, with the maximal stimulation observed with 8-OH-DPAT taken as 100%. The concentration–response curves of the agonistic activity were analyzed by GraphPad as reported above.[26] The maximum percentage of stimulation of [^{35}S]GTPγS binding (E_{max}) achieved for each drug, and the concentration required to obtain 50% of E_{max} (pD_2 = −log10 [EC_{50}]) were evaluated.

In functional studies, responses were expressed as a percentage of the maximal contraction observed in the agonist concentration–response curves, taken as a control, which were analyzed by pharmacological computer programs. pA_2 values were calculated according to the method of Arunlakshana and Schild from the dose ratios at EC_{50} values of the agonists calculated at three different antagonist concentrations. Each concentration was tested at least four times, and the Schild plots were constrained to a slope of −1 as required by theory. pK_b values were calculated according to the method of van Rossum at one or two concentrations.[27]

Docking analysis by molecular modeling

The (*R*/*S*)-flesinoxan, (*R*/*S*)-WB 4101 and the (*R*)-**1** and (*S*)-**1** enantiomers were built, parameterised (Gasteiger–Huckel method) and energy minimised within MOE using MMFF94 forcefield.[28] For all compounds, the protonated form was considered for the *in silico* analyses. In the absence of crystallographic data for the 5-HT_{1A} receptor, the theoretical model of the human 5-HT_{1A} previously built by us has been used for docking simulations.[15] An alpha1_D theoretical model has been built starting from the X-ray structure of the β_2-adrenoreceptor (pdb code 2RH1), by applying the homology modeling strategy already described by us for the 5-HT_{1A} receptor model. Briefly, since most of the key residues characteristic of GPCRs are conserved in the α_{1D}-adrenoreceptor, an α_{1D} homology model has been generated, starting from the X-ray structure of human β_2-adrenoreceptor (PDB code: 2RH1; resolution = 2.40 Å), in complex with a partial inverse agonist compound.[29] The amino acid sequence of the α_{1D}-adrenoreceptor (P25100) was retrieved from the SWISSPROT database[30] while the three-dimensional structure coordinate file of the GPCR template was obtained from the Protein Data Bank.[31] The amino acid sequences of α_{1D} TM helices were aligned with the corresponding residues of 2RH1, on the basis of the Blosum62 matrix (MOE software). The connecting loops were constructed by the loop search method implemented in MOE. The energy minimization was carried out by 1000 steps of steepest descent followed by conjugate gradient minimization until the rms gradient of the potential energy was less than 0.1 kcal mol^{-1} Å^{-1}. The assessment of the final obtained model was performed using Ramachandran plots, generated within MOE.

Docking studies were subsequently performed, according to the following protocol. The binding site of the ligand in the 5-HT_{1A} receptor was determined starting from the fact that, for the ligand activity, formation of the salt bridge between the protonated piperazine nitrogen on the ligand and Asp116 is necessary.[32–34]

On the other hand, the α_{1d}-adrenoreceptor binding site has been determined by taking especially into account the conserved residues highlighted by a comparison with the β_2-adrenoreceptor and 5-HT_{1A} binding site.

Each isomer was docked into the putative ligand binding site by means of the Surflex docking module implemented in Sybyl-X1.0.[35] Then, for all the compounds, the best docking geometries (selected on the basis of the SurFlex scoring functions) were refined by ligand–receptor complex energy minimization (CHARMM27) by means of the MOE software. To verify the reliability of the derived docking poses, the obtained ligand/receptor complexes were further investigated by docking calculations (10 run), using MOE-Dock (Genetic algorithm; applied on the poses already located into the putative 5-HT1A or α_{1d}-adrenoreceptor). The conformers showing lower energy scoring functions and rmsd values (with respect to the starting poses) were selected as the most stable and discussed here.

Conclusions

In this paper, the enantiomers of (±)-**1** were prepared and evaluated for *in vitro* 5-HT_{1A} and α_1 receptor affinity by binding and functional assays. Results indicate that the two enantiomers are almost equally potent at 5-HT_{1A} and α_1 receptor systems. *In silico* results were consistent with the pharmacological findings as they indicated that the binding modes of the two enantiomers were almost identical.

Acknowledgements

We thank Dr. Cristian Siligardi for technical support.

Notes and references

1 J. P. Hieble, D. B. Bylund, D. E. Clarke, D. C. Eikenburg, S. Z. Langer, R. J. Lefkowitz, K. P. Minneman and R. R. Ruffolo Jr, *Pharmacol. Rev.*, 1995, **47**, 267–270.
2 A. P. Ford, T. J. Williams, D. R. Blue and D. E. Clarke, *Trends Pharmacol. Sci.*, 1994, **15**, 167–170.
3 M. G. Bock and M. A. Patane, *Annu. Rep. Med. Chem.*, 2000, 221–230.
4 E. Meller, *Biochim. Biophys. Acta*, 2007, **1773**, 691–693.
5 I. Misane and S. O. Ogren, *Neuropsychopharmacology*, 2003, **28**, 253–264.
6 S. Trumpp-Kallmeyer, J. Hoflack, A. Bruinvels and M. Hibert, *J. Med. Chem.*, 1992, **35**, 3448–3462.
7 L. Brasili, C. Sorbi, S. Franchini, M. Manicardi, P. Angeli, G. Marucci, A. Leonardi and E. Poggesi, *J. Med. Chem.*, 2003, **46**, 1504–1511.

8 S. Franchini, A. Tait, A. Prandi, C. Sorbi, R. Gallesi, M. Buccioni, G. Marucci, C. De Stefani, A. Cilia and L. Brasili, *ChemMedChem*, 2009, **4**, 196–203.

9 I. A. Cliffe, C. I. Brightwell, A. Fletcher, E. A. Forster, H. L. Mansell, Y. Reilly, C. Routledge and A. C. White, *J. Med. Chem.*, 1993, **36**, 1509–1510.

10 A. Fletcher, D. J. Bill, S. J. Bill, I. A. Cliffe, G. M. Dover, E. A. Forster, J. T. Haskins, D. Jones, H. L. Mansell and Y. Reilly, *Eur. J. Pharmacol.*, 1993, **237**, 283–291.

11 W. Kuipers, C. G. Kruse, I. van Wijngaarden, P. J. Standaar, M. T. Tulp, N. Veldman, A. L. Spek and A. P. IJzerman, *J. Med. Chem.*, 1997, **40**, 300–312.

12 J. Gommans, T. H. Hijzen, R. A. Maes, J. Mos and B. Olivier, *Eur. J. Pharmacol.*, 1995, **284**, 135–140.

13 V. Andrisano, G. Marucci, C. Melchiorre and V. Tumiatti, *Chirality*, 1992, **4**, 16–20.

14 L. Fumagalli, M. Pallavicini, R. Budriesi, C. Bolchi, M. Canovi, A. Chiarini, G. Chiodini, M. Gobbi, P. Laurino, M. Micucci, V. Straniero and E. Valoti, *J. Med. Chem.*, 2013, **56**, 6402–6412.

15 A. Prandi, S. Franchini, L. I. Manasieva, P. Fossa, E. Cichero, G. Marucci, M. Buccioni, A. Cilia, L. Pirona and L. Brasili, *J. Med. Chem.*, 2012, **55**, 23–36.

16 J. F. Gerster, S. R. Rohlfing, S. E. Pecore, R. M. Winandy, R. M. Stern, J. E. Landmesser, R. A. Olsen and W. B. Gleason, *J. Med. Chem.*, 1987, **30**, 839–843.

17 C. Bolchi, P. Catalano, L. Fumagalli, M. Gobbi, M. Pallavicini, A. Pedretti, L. Villa, G. Vistoli and E. Valoti, *Bioorg. Med. Chem.*, 2004, **12**, 4937–4951.

18 I. Skelin, F. Yamane and M. Diksic, *Neurochem. Int.*, 2008, **53**, 236–243.

19 A. F. Beecham, *J. Am. Chem. Soc.*, 1957, **79**, 3257–3261.

20 M. Eltze, R. Boer, K. H. Sanders and N. Kolassa, *Eur. J. Pharmacol.*, 1991, **202**, 33–44.

21 F. N. Ko, J. H. Guh, S. M. Yu, Y. S. Hou, Y. C. Wu and C. M. Teng, *Br. J. Pharmacol.*, 1994, **112**, 1174–1180.

22 S. A. Buckner, K. W. Oheim, P. A. Morse, S. M. Knepper and A. A. Hancock, *Eur. J. Pharmacol.*, 1996, **297**, 241–248.

23 R. Testa, C. Taddei, E. Poggesi, C. Destefani, S. Cotecchia, J. P. Hieble, A. C. Sulpizio, D. Naselsky and D. Bergsma, *et al.*, *Pharmacol. Commun.*, 1995, **6**, 79–86.

24 J. A. Stanton and M. S. Beer, *Eur. J. Pharmacol.*, 1997, **320**, 267–275.

25 C. Yung-Chi and W. H. Prusoff, *Biochem. Pharmacol.*, 1973, **22**, 3099–3108.

26 A. De Lean, P. J. Munson and D. Rodbard, *Am. J. Physiol.*, 1978, **235**, E97–E102.

27 J. M. van Rossum, *Arch. Int. Pharmacodyn. Ther.*, 1963, **143**, 299–330.

28 *MOE*, Chemical Computing Group Inc., Montreal H3A 2R7, Canada, 2011.

29 V. Cherezov, D. M. Rosenbaum, M. A. Hanson, S. G. F. Rasmussen, F. S. Thian, T. S. Kobilka, H.-J. Choi, P. Kuhn, W. I. Weis, B. K. Kobilka and R. C. Stevens, *Science*, 2007, **318**, 1258–1265.

30 A. Bairoch and R. Apweiler, *Nucleic Acids Res.*, 2000, **28**, 45–48.

31 H. M. Berman, J. Westbrook, Z. Feng, G. Gilliland, T. N. Bhat, H. Weissig, I. N. Shindyalov and P. E. Bourne, *Nucleic Acids Res.*, 2000, **28**, 235–242.

32 C. D. Strader, M. R. Candelore, W. S. Hill, R. A. Dixon and I. S. Sigal, *J. Biol. Chem.*, 1989, **264**, 16470–16477.

33 X. M. Guan, S. J. Peroutka and B. K. Kobilka, *Mol. Pharmacol.*, 1992, **41**, 695–698.

34 G. Liapakis, J. A. Ballesteros, S. Papachristou, W. C. Chan, X. Chen and J. A. Javitch, *J. Biol. Chem.*, 2000, **275**, 37779–37788.

35 Sybyl X 1.0 Tripos Inc 1699 South Hanley Road. St Louis. Missouri. 63144. USA.

